Will Piecewise Continuous Echo Spacing Adversely Affect The T_2 Distribution?

T. A. Bjarnason[1]

[1]Electrical & Computer Engineering, University of Calgary, Calgary, AB, Canada

Introduction: The Poon-Henkelman implementation of the multi-echo imaging pulse sequence can be used to measure T_2 decay curves in brain [1]. This pulse sequence is characterized by crusher and read gradients; both of which look similar to gradients used for diffusion imaging. Consequently, improper choice of echo spacing can introduce spurious peaks into the T_2 distribution [2]. Three T_2 components are consistently found in healthy white matter at 1.5 T: i) a minor, myelin water, component with a short T_2 time between 10-55 ms, ii) a major component, intra/extracellular water, with a T_2 time between 70-95 ms, and iii) a component with a T_2 time greater than 1000 ms attributed to cerebrospinal fluid [3]. In order to sufficiently sample both short and long components, one can use a piecewise continuous 48 echo acquisition scheme that collects out to 1120 ms by changing the echo spacing from 10 to 50 ms after the 32nd echo [4]. This acquisition scheme provides better defined T_2 distributions because potential components of the order of 500 ms, which might occur in pathology, are more properly sampled; thus better defining these longer components, and in turn relieving the burden of fitting undersampled data on the shorter components [4]. The following work provides simulations supporting the use of piecewise continuous echo spacing for acquiring T_2 relaxation data that adequately samples both short components on the order of 10 ms and long components on the order of 500 ms. Simulations were performed assuming three mono-exponential cases: 200, 500, and 1000 ms.

Methods: A simple attenuation equation in magnetic resonance due to the diffusion properties of water with the existence of magnetic field gradients is [5] $M=M(0)\exp(-bD)$, where $b=(\gamma\lambda G)^2(\Lambda-\lambda/3)$. The change of diffusion literature's variables is intentional so that the duration of the pulse will not be confused with the Kroeneker delta. All pulses are assumed to be rectangular in shape. A mathematical description of the effects of diffusion on the 48 multi-echo pulse sequence in regards to matching sets of four crushers constantly decreasing by G/N following every second pair is presented in Eq. 1 where: G is the initial crusher strength, N is half the total echoes, n is echo number, t_e is the initial echo spacing and the secondary echo spacing is assumed to be 5 times t_e, m=n-32, $\delta_{i,j}^{\ k}$ is the Kroneker delta that has the value of unity when the condition in the subscript is true and zero if false, and b_c is the b-factor of the first pair of crusher gradients. The case of constant read gradients is shown in Eq. 2, where b_{r1} and b_{r2} are the b-values of the first 32 and final 16 read gradients. As a result, the measured T_2 components will be shifted as $1/T_2^{obs}=1/T_2+1/c_1$ for the primary echo spacing and $1/T_2^{obs}=1/T_2+1/c_2$ for the secondary echo spacing. The realistic case of assuming both read and crusher gradients are shown in Eq. 3. For simulation purposes, the diffusion rate of water at room temperature was assumed, the default initial crusher gradient was 0.023 T•m^{-1}, the default read gradient was 0.01 T•m^{-1}, the duration of the crusher and read gradients were 2 ms and 4 ms, and the time between the beginnings of the crusher and read gradients were 2.13 ms and $t_e/2$. The resulting curves were fit using regularized NNLS with the energy constraint of $1.02\chi_{min}^2\le\chi^2\le1.025\chi_{min}^2$ [6].

$$M(t_n)=\begin{cases} M(0)\exp\left[-nt_e/T_2\right]\times\prod_{i=0}^{n-1}\left[\delta_{i,odd}^{k}f_{odd}(i)+\delta_{i,even}^{k}f_{even}(i)\right] & \text{for } 1\le n\le 32 \\ M(t_{32})\exp\left[-5mt_e/T_2\right]\times\prod_{i=32}^{n-1}\left[\delta_{i,odd}^{k}f_{odd}(i)+\delta_{i,even}^{k}f_{even}(i)\right] & \text{for } 33\le n\le 48 \end{cases}; \quad \begin{aligned} f_{odd}(i)&=\exp\left[-Db_c\left(\left[N-i/2+i/2\right]/N\right)^2\right] \\ f_{even}(i)&=\exp\left[-Db_c\left(\left[N-i/2\right]/N\right)^2\right] \end{aligned} \tag{1}$$

$$M(t_n)=\begin{cases} M(0)\exp\left[-nt_e/T_2\right]\exp\left[-nt_e/c_1\right] & \text{for } 1\le n\le 32 \\ M(t_{32})\exp\left[-5mt_e/T_2\right]\exp\left[-5mt_e/c_2\right] & \text{for } 33\le n\le 48 \end{cases}; \quad \begin{aligned} 1/c_1&=Db_{r1}/2\Lambda \\ 1/c_2&=Db_{r2}/10\Lambda \end{aligned} \tag{2}$$

$$M(t_n)=\begin{cases} M(0)\exp\left[-nt_e\left(1/T_2+1/c_1\right)\right]\times\prod_{i=0}^{n-1}\left[\delta_{i,odd}^{k}f_{odd}(i)+\delta_{i,even}^{k}f_{even}(i)\right] & \text{for } 1\le n\le 32 \\ M(t_{32})\exp\left[-5mt_e\left(1/T_2+1/c_2\right)\right]\times\prod_{i=32}^{n-1}\left[\delta_{i,odd}^{k}f_{odd}(i)+\delta_{i,even}^{k}f_{even}(i)\right] & \text{for } 33\le n\le 48 \end{cases} \tag{3}$$

Results: The simulation results are shown in the Figs. Constantly decreasing crusher simulations are shown in Fig. 1 where $b_c=5.6\times10^3$ s•m^{-2}, $b_c=2.8\times10^6$ s•m^{-2}, and $b_c=2.8\times10^7$ s•m^{-2} shown in panels A, B, and C; spurious peaks were introduced for the larger two b-values. Fig. 2 represents read gradients with b-values for the first 32 and final 16 gradients: $b_{r1}=10^4$ s•m^{-2} and $b_{r2}=7\times10^4$ s•m^{-2} for A, $b_{r1}=5\times10^6$ s•m^{-2} and $b_{r2}=3.5\times10^7$ s•m^{-2} for B, and $b_{r1}=5\times10^7$ s•m^{-2} and $b_{r2}=2.5\times10^8$ s•m^{-2} for C. It is evident that only b_{r1} affects the distribution. Shifts of the peaks are noted, and can be described by T_2^{obs}. For Fig. 3 the relevant parameters are: $b_c=5.6\times10^3$ s•m^{-2} and $b_{r1}=10^4$ s•m^{-2} for A, $b_c=2.8\times10^6$ s•m^{-2} and 5×10^6 s•m^{-2} for B, and $b_c=2.8\times10^7$ s•m^{-2} and $b_{r1}=5\times10^7$ s•m^{-2} for C.

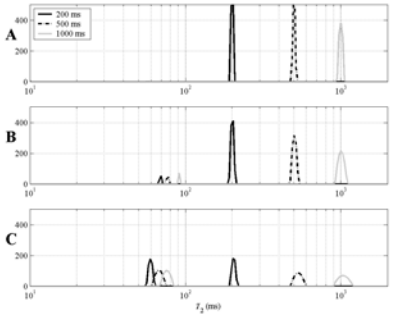

Fig. 1: *T_2 distributions for matching sets of decreasing crushers*.

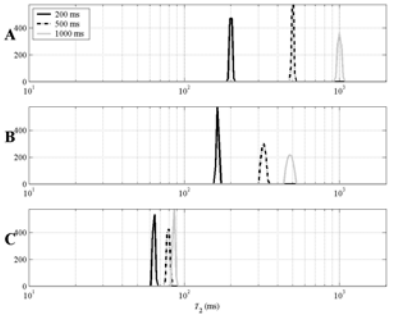

Fig. 2: *T_2 distributions for constant read gradients*.

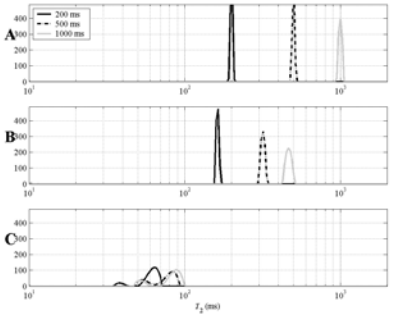

Fig. 3: *T_2 distributions for both constant read gradients and matching sets of decreasing crushers*.

Discussion: Realistic scanner parameters are shown in A of the Figs. The crusher gradients of B and C are beyond our scanner capabilities, while B of the read gradients could be possible if one were to use maximum read gradients. However, this case is unlikely because field of view scales inversely with the gradient strength.

Conclusion: Three cases of diffusion weighting resulting from a piecewise continuous 48 echo acquisition were explored. The contribution of diffusion weighting on the T_2 distributions were negligible given realistic scanner parameters; spurious peaks were not created. Hence, adverse effects such as additional peaks in the T_2 distribution outside of those typically found in healthy white matter are not an artifact of the acquisition scheme, but are representative of additional, possibly pathological, microstructures.

1. Poon & Henkelman. JMRI 2:541-52 (1992)
2. Does & Gore. NMR Biomed 13:1-7 (2000)
3. MacKay *et al*. MRM 31:673-7 (1994)
4. Skinner. MSc Thesis. UBC. 2001
5. Stejskal & Tanner. J Chem Phys 42:288-92 (1964)
6. Whittall & MacKay. JMR 84:134-52 (1989)

Acknowledgements: Thank you Dr. Alex MacKay for your assistance. This work was funded in part by the Multiple Sclerosis Society of Canada.